Appl. Phys. B (2014) 114:551–555
DOI 10.1007/s00340-013-5559-2

Applied Physics B
Lasers and Optics

Optical excitation study on the efficiency droop behaviors of InGaN/GaN multiple-quantum-well structures

**Yuanping Sun · Hongying Guo · Lihua Jin ·
Yong-Hoon Cho · E.-K. Suh · H. J. Lee ·
R. J. Choi · Y. B. Hahn**

Received: 19 November 2012 / Accepted: 18 June 2013 / Published online: 3 July 2013

Abstract Efficiency droop is generally observed in electroluminescence under high current injection. Optical characterization on efficiency droop in InGaN/GaN multiple-quantum-well structures has been conducted at 12 K. Clear droop behaviors were observed for the sample excited by above-bandgap excitation of GaN with pulse laser. The results show that dislocation is not the crucial factor to droop under high carrier density injection, and Auger recombination just slightly affects the efficiency. The radiative recombination may be mainly affected by a multi-carrier-related process (diffusion and drift with a factor of $n^{3.5}$ and $n^{5.5}$) at the interface between GaN barrier and InGaN well.

The cool and efficient white LEDs, which based on the III-Nitride light-emitting diodes (LEDs), have been expected to replace the traditional incandescent bulbs and fluorescent tubes in recent years to save the numerous energy consumption wasted by heat generation [1, 2]. But, a severe obstacle to future solid state lighting applications of such devices emerges when high-drive current is applied to get a very high light output, and the internal quantum efficiency decreased dramatically. This phenomenon is generally called as efficiency droop [3], which means a reduction in electroluminescence efficiency with increasing current density. Although many studies have been conducted to find the origination of this problem, the underlying mechanisms still remain under controversy. Besides delocalization of carriers [4], thermal effects [5], and high density of dislocation [4, 6], most of researchers contribute this to the Auger recombination [7–9] and carrier leakage caused by polarization effects [10–12]. The theoretical calculations also suggest that the defect- or phonon-assisted Auger recombination should be responsible for the efficiency droop [13]. In fact, most of the researches are based on electrical carrier injection (electroluminescence, EL) instead of photon-excited luminescence (photoluminescence, PL) for the difficult explanation of experimental results. The reported PL efficiency droop has only been shown in resonant PL experiment [7]. But the photon excitation is a useful tool to study the carrier dynamics, which may provide better understandings to the origination of efficiency droop. In this letter, we report the photon-excited efficiency droop behaviors in InGaN multiple-quantum-well structures (MQWs) by different laser sources. A clear efficiency droop behavior was observed when we excited the sample by pulse laser with laser energy above GaN bandgap, which is attributed to the multi-carrier recombination processes.

The studied InGaN/GaN MQWs sample has the general structures present in III-nitride LEDs, which were grown on *c*-plane sapphire substrates by horizontal metal–organic chemical vapor deposition (MOCVD). Trimethylgallium

Y. Sun (✉) · H. Guo
Institute of Science and Technology for Opto-Electronic Information, Yantai University, Yantai 264005, China
e-mail: ypsun@ytu.edu.cn

L. Jin · Y.-H. Cho
Department of Physics and Graduate School of Nanoscience and Technology (WCU), Korea Advanced Institute of Science and Technology (KAIST), Daejeon 305-701, Republic of Korea

E.-K. Suh · H. J. Lee
Department of Semiconductor Science and Technology and Semiconductor Physics Research Center, Chonbuk National University, Chonju 561-756, Korea

R. J. Choi · Y. B. Hahn
School of Chemical Engineering, Chonbuk National University, Chonju 561-756, Korea

(TMGa), trimethylindium (TMIn), ammonia, and silane were used as the precursors of Ga, In, N, and Si, respectively. Nitrogen was used as a carrier gas for the sources. After thermal cleaning of the substrate in hydrogen ambient for 10 min at 1,100 °C, a 25-nm-thick GaN nucleation layer was grown on *c*-plane sapphire substrates at 560 °C and followed by a 1-μm Si-doped GaN layer at 1,130 °C. Five periods of InGaN/GaN QWs were grown at 795 °C and then a 100-nm-thick GaN capping layer was grown at 1,050 °C. The average indium content in well layers estimated from the flux of TMIn is around 0.24. The thickness of barrier and well layers was about 8 and 3 nm, respectively. PL measurements were performed with a He-cooling stage operating at 12 K. Different excitation sources are selected to excite the samples below and above GaN bandgap. A second harmonic pulsed Ti: sapphire laser at the wavelength of 354 and 370 nm was used to excite samples under pulsed conditions (repetition rate 0.5 MHz), while a He–Cd laser at 325 nm and a semiconductor laser diode at 405 nm were used as continuous excitation sources (CW laser). The laser intensity was changed by neutral density filters with a power range from 1 to 700 μW. The diameter of laser excitation spot was focused to ~0.2 mm, which corresponds to a photon density of about 1.13×10^{13}, 1.18×10^{13}, 1.30×10^{15}, and $1.62 \times 10^{13}/\mathrm{cm}^2$ per microwatt for pulsed laser of 354 and 370 nm, CW laser of 325 and 405 nm, respectively.

Figure 1 shows the normalized PL spectra with an excitation power of 5 and 700 μW, which the sample were excited by the pulse laser at 354, 370 nm and CW laser at 325, 405 nm at 12 K, respectively. The main emission peaks lie at 473 and 467 nm for different lasers with a power of 5 μW, respectively. When the sample is excited by lasers with power of 700 μW, the emission peak lies at 467 and 472 nm, respectively. So, if the sample was excited below GaN bandgap by pulse laser and by CW lasers, the sample shows a relatively stable main emission peaks (the blue-shift is <6 meV) with the power varied from 5 to 700 μW. But for the pulse laser excitation above GaN bandgap, it brought a blue-shift of ~28 meV to the main emission peak in the same power range. The inset of Fig. 1 shows the peak shift of main emissions in the excitation power range from 5 to 700 μW.

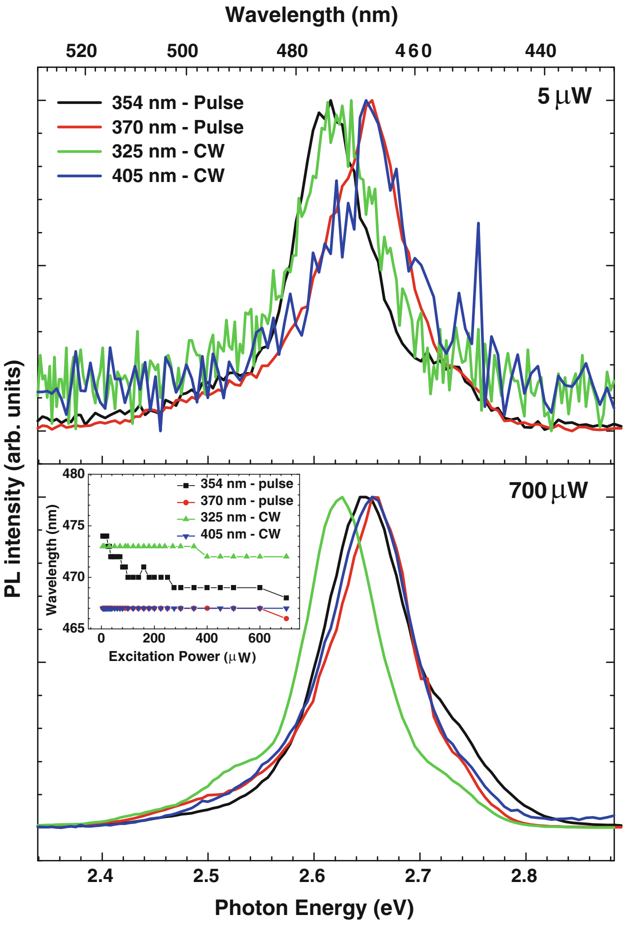

Fig. 1 Power-dependent PL spectra at 12 K, which is excited with a power of 5 and 700 μW by pulse laser at 354, 370 nm and CW laser at 325, 405 nm. The inset shows the main emission peak shift with powers

To study the internal efficiency changes of InGaN sample excited by different laser sources, power-dependent PL spectra have been integrated from 430 to 530 nm, which covers all the emissions from InGaN well layers. The integrated intensity with excitation power for different laser sources are shown in Fig. 2. The carrier density in the active region can be described by the carrier rate equation

$$\frac{dn}{dt} = G(t) - An - Bn^2 - Cn^3 \qquad (1)$$

where $G(t)$ is the carrier generation density, An is the nonradiative recombination rate, Bn^2 is the bimolecular radiative recombination rate and Cn^3 is also a nonradiative recombination rate with 3 particles involved. The carrier generation density $G(t)$ is proportional to the excitation power P, by considering both the radiative and nonradiative recombination together, the integrated PL intensity I (corresponds to radiative recombination) should be a function of excitation power P

$$I \sim P^{\gamma} \qquad (2)$$

According to this formula, if the first nonradiative recombination An (Shockley-Read-Hall recombination, SRH) in formula (1) is dominant, γ should be close to 2; if radiative recombination Bn^2 is dominant, γ should be close to 1; and γ is close to 2/3, if the nonradiative recombination Cn^3 is dominant.

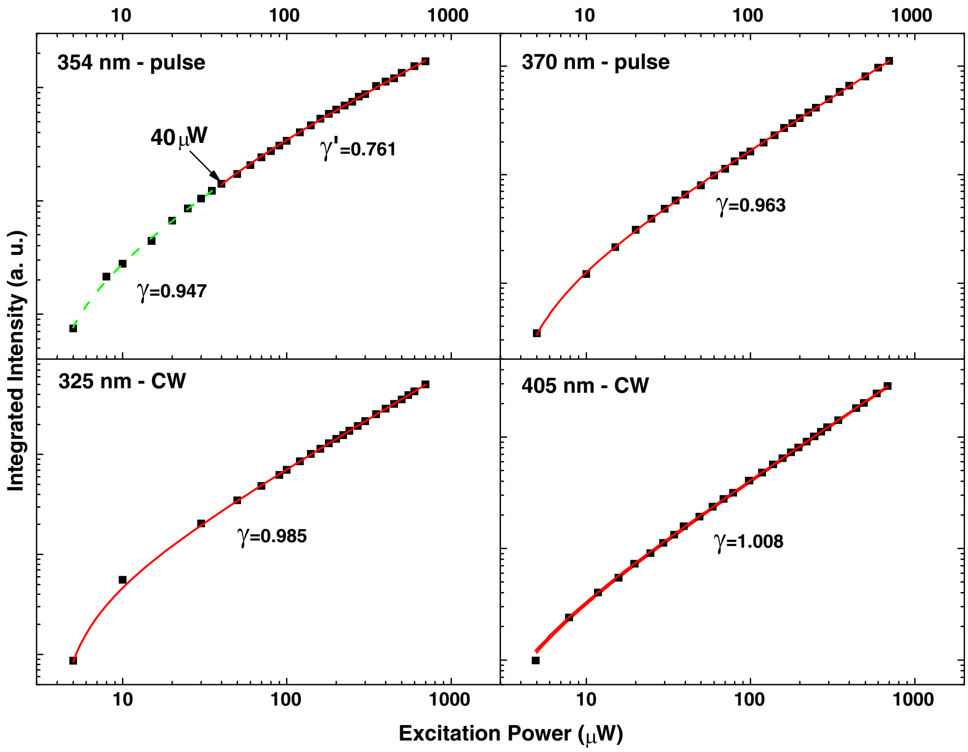

Fig. 2 The integrated intensity changes with excitation power for different excitation sources at 12 K. The *dots* are experimental data, and lines are fitting results according to formula (2)

All the integrated intensities have been fitted by using formula (2), and the results are shown in Fig. 2. A single γ in formula (2) can be used to fit the experimental data well except for the data obtained by 354 nm pulse laser excitation. To avoid the deviation between the model-fitting and experimental data, we divided this group of data into two parts and fit them separately to get the best fitting as in Fig. 2a. The fitted γ is 0.947, 0.963, 0.985 and 1.008 for the excitation source of 354 (lower power excitation part), 370 nm pulse laser and 325, 405 nm CW laser, respectively, which shows a slight increase in the value around 1. As we have pointed above, γ should be close to 1 if the radiative recombination is dominant. So, the radiative recombination is dominant when the sample were excited by low power of 354 nm pulse laser and three other excitation lasers, in which the nonradiative recombination is suppressed. It is well known that all the defect-related recombination is frozen out at lower temperature (in this study, 12 K), and the radiative recombination is dominant. But for the high power range of 354 nm pulse laser excitation, the fitted parameter γ is just 0.761, which is closer to the value limit of 3-particle nonradiative recombination (Auger recombination or carrier leakage).

Figure 3 shows the normalized efficiency decay of sample excited by four different laser sources. Efficiency droop behavior is more obvious when excited the sample by 354 nm pulse laser than by other laser sources. The efficiency increases with the increase in excitation power to 40 μW, and then it decreases to its 53 % at the excitation power of 700 μW. It also should be noted that this point is just the dividing point when we fit the data with formula (2) as shown in Fig. 2. So, this is a turning point that nonradiative recombination begin to dominate. For the efficiency behavior excited by 370 nm pulse laser, this point is not clear and the efficiency drops to 90.6 % of the maximum when the power increases to 700 μW. While for the excitation by CW lasers, the efficiency increases to its maximum and then keeps almost at a constant. This phenomenon is well in accordance with the above γ values. So, exciting the sample by pulse laser with the energy above GaN bandgap is the best optical method to study the efficiency droop behavior in InGaN MQWs.

Generally, the efficiency droop behavior is thought to be caused by Auger recombination and/or carrier leakage. Based on the Auger recombination theory, the efficiency droop can be reduced by spreading the carriers over more materials since Auger recombination rate is proportional to the cube of the carrier's density. But the improvement is not so pronounced at high current density that the new structure is less efficient than the standard one at low current density [14, 15]. Based on the carrier leakage analysis, Schubert's team fabricated the polarization-matched MQW LEDs to reduce the efficiency droop. The reported results show that the power output is raised by 25 % at high currents [10]. From the inset of Fig. 1, we can find that the main emission peak shows the largest blueshift when the sample was excited by 354 nm pulse laser within a power range from 5 to 700 μW. It is well known

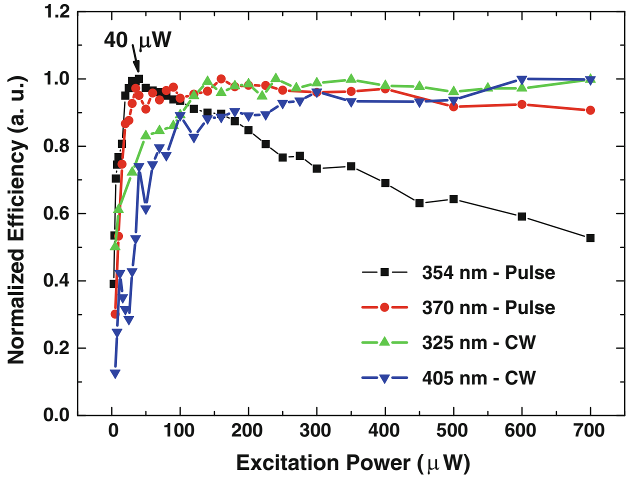

Fig. 3 Normalized efficiency evaluation with excited powers for different exciting laser sources at 12 K

that large internal electric fields exist in III-nitride MQW materials due to the large spontaneous polarization [16]. High carrier density will screen the internal electric fields and lead to the blue-shift of emission peak. For our case, it corresponds to the 354 nm pulse laser excitation which has the largest transient carrier density. The effective screening of internal electric fields caused the largest blue-shift of emission peaks, which corresponds to the most serious efficiency droop (Fig. 3).

Also, because of the high density of carriers, the Auger recombination may also plays an important role in the efficiency droop. But when we excited the sample with 370 nm pulse laser, the droop behavior is not obvious. The difference in carrier density between 354 and 370 nm pulse laser is small, but the droop behavior shows large difference. This phenomenon may imply that the droop is related to the internal electric field in III-nitride samples more than the Auger recombination. The screening of internal electric field will cause the efficiency droop. On the other hand, the Auger recombination is temperature dependent [17]. At low temperature (12 K in our cases), the Auger recombination may not be dominant. In fact, recent study also supported this explanation, in which the Auger recombination coefficient is decided to be $1.8 \pm 0.2 \times 10^{-31}$ cm^6/s [18]. On the other hand, by comparing the droop behaviors excited by 354 and 370 nm pulse laser, the carrier's generation in barriers and transport from the barrier to well layers will influence the efficiency more than the carrier's recombination in the wells, which may imply that the carriers' loss during the transport instead of Auger recombination is the origin of efficiency droop. Also, from Fig. 3, we can find that the efficiency droop behavior may not be related to the defect in samples, which the fitting parameter γ should be larger than 1. This can be explained by the frozen out of defects at low temperature.

The carriers' leakage across the heterojunction between the active layer and p-confining layer can arise due to either drift [19] or diffusion [20], as have been found in InGaAsP light-emitting sources [21]. Depending on the p-doping level of confining layer, the drift leakage current or the diffusion leakage current dominates. By considering the p-doping level in GaN materials ($\sim 10^{17}$/cm^3) [22–24], the electric fields are large and the drift leakage current may dominate [19]. If we let Δn be the density of conduction electrons in active layer whose energy exceeds the conduction band edge of p-confining layer, the leakage current density caused by diffusion is [25]

$$J_{\text{diff}} = eD_n \Delta n / w \tag{3}$$

where D_n is the electron diffusivity in the p-confining layer, and w is its thickness. The total current density in p-confining layer is comprised of electron leakage current and injected hole current, which can be written as

$$J_{\text{drift}} = \mu_e \Delta n E \tag{4}$$

and

$$J_{\text{inject}} = \mu_p (\Delta n + p) E \tag{5}$$

where E is the electric field, p the acceptor density, and μ_e and μ_p the electron and hole mobilities in p-confining layer, respectively. Because Δn is much smaller than p, we then have

$$J_{\text{drift}} = \frac{\mu_e \Delta n}{\mu_p p} J_{\text{inject}} \tag{6}$$

If the injection current density varies as n^2 (since the injected hole current is dominated by the bimolecular term αn^2 [26]) and Δn varies as $n^{3.5}$, then, we can have $J_{\text{diff}} \propto n^{3.5}$ and $J_{\text{drift}} \propto n^{5.5}$, in which the carrier rate equation will contain a term [21]

$$R_{\text{leakage}} = \begin{cases} Dn^{3.5}, & \text{if diffusion dominates} \\ Dn^{5.5}, & \text{if drift dominates} \end{cases} \tag{7}$$

which will lead to a carrier rate equation

$$\frac{dn}{dt} = G(t) - An - Bn^2 - Cn^3 - Dn^\theta \tag{8}$$

the θ is 3.5 or 5.5 depending on the domination of diffusion or drift. According to formula (8), we conducted a simulation on the data obtained by the excitation of 354 nm pulse laser (See in Fig. 2), and the results are shown in Fig. 4. The solid and dashed curves represent the fitting result by using Auger and leakage model, respectively. We can see from the figure that the leakage model gives the best description of experimental data for all of the power range. A calculated θ value of 3.95 is obtained, which may imply the domination of carrier leakage. On the other hand,

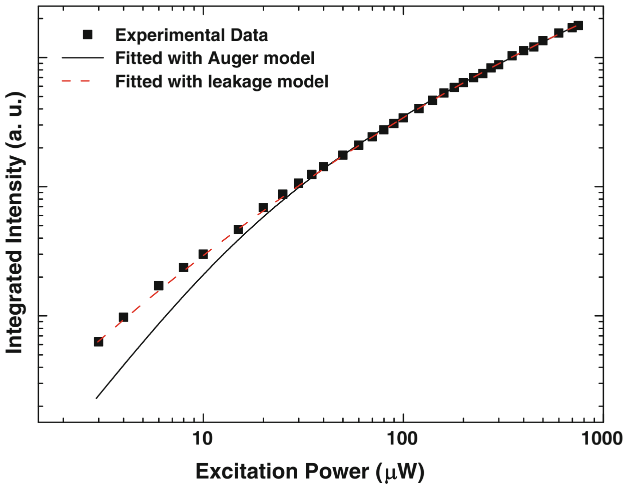

Fig. 4 Fitted results on the integrated intensity data obtained by the excitation with 354 nm pulse laser (See in Fig. 2). The *dots* are experimental data, the *solid* and *dashed line* represent the fitted curve with Auger (Cn^3) and leakage model (Dn^0) in formula (8), respectively

the fitted curves of the two models are almost same in the range that efficiency droop happened. It is still not clear to distinguish the real reason for efficiency droop [27].

In conclusion, we have studied the efficiency droop behaviors of InGaN MQW structures by PL at 12 K with different laser excitation. Exciting the sample at low temperature (12 K) by pulse laser with the energy larger than GaN bandgap is the best optical method to study the efficiency droop behavior. The droop is not related to the defect density in sample; the Auger recombination just slightly affect the efficiency droop [28] (3-particles). But another multi-carrier recombination process (more than 3), such as carrier leakage at the interface between GaN barrier and InGaN well (diffusion and drift with an factor of $n^{3.5}$ and $n^{5.5}$), could be the reason for the efficiency droop in III-nitride MQWs structures.

Acknowledgments This work is supported by the National Natural Science Foundation of China (Grant number: 11174241), Natural Science Foundation of Shandong Province (No. 2009VRA06063), and the Natural Science Foundation for Distinguished Young Scholars of Shandong province (No. 2008JQB01028). The work at KAIST was supported by the WCU Program (No. R31-2008-000-10071-0) funded by the Ministry of Education, Science and Technology (Korea).

References

1. D.G. Morrison, Electron. Des. **50**(11), 66 (2002)
2. K. Bando, K. Sakano, Y. Noguchi, Y. Shimizu, J. Light Visual Environ. **22**(1), 2 (1998)
3. T. Mukai, M. Yamada, S. Nakamura, Jpn. J. Appl. Phys. **1**(38), 3976 (1999)
4. K. Akita, T. Kyono, Y. Yoshizumi, H. Kitabayashi, K. Katayama, J. Appl. Phys. **101**(3), 033104 (2007)
5. A.A. Efremov, N.I. Bochkareva, R.I. Gorbunov, D.A. Lavrinovich, Y.T. Rebane, D.V. Tarkhin, Y.G. Shreter, *Semiconductors ±40/5* (2006) 605
6. B. Monemar, B.E. Sernelius, Appl. Phys. Lett. **91**(18), 181103 (2007)
7. Y.C. Shen, G.O. Mueller, S. Watanabe, N.F. Gardner, A. Munkholm, M.R. Krames, Appl. Phys. Lett. **91**(14), 141101 (2007)
8. K.T. Delaney, P. Rinke, C.G. Van de Walle, Appl. Phys. Lett. **94**(19), 191109 (2009)
9. S.H. Yen, M.C. Tsai, M.L. Tsai, Y.J. Shen, T.C. Hsu, Y.K. Kuo, Appl. Phys. Mater. **97**(3), 705 (2009)
10. M.F. Schubert, J. Xu, J.K. Kim, E.F. Schubert, M.H. Kim, S. Yoon, S.M. Lee, C. Sone, T. Sakong, Y. Park, Appl. Phys. Lett. **93**(4), 041102 (2008)
11. M.F. Schubert, Q. Dai, J. Xu, J.K. Kim, E.F. Schubert, Appl. Phys. Lett. **95**(19), 191105 (2009)
12. M.F. Schubert, J.R. Xu, Q. Dai, F.W. Mont, J.K. Kim, E.F. Schubert, Appl. Phys. Lett. **94**(8), 081114 (2009)
13. J. Hader, J.V. Moloney, B. Pasenow, S.W. Koch, M. Sabathil, N. Linder, S. Lutgen, Appl. Phys. Lett. **92**(26), 261103 (2008)
14. N.F. Gardner, G.O. Muller, Y.C. Shen, G. Chen, S. Watanabe, W. Gotz, M.R. Krames, Appl. Phys. Lett. **91**(24), 243506 (2007)
15. A. David, M.J. Grundmann, J.F. Kaeding, N.F. Gardner, T.G. Mihopoulos, M.R. Krames, Appl. Phys. Lett. **92**(5), 053502 (2008)
16. U.M.E. Christmas, A.D. Andreev, D.A. Faux, J. Appl. Phys. **98**(7), 073522 (2005)
17. D.G. Gevaux, A.M. Green, C.C. Phillips, I. Vurgaftman, W.W. Bewley, C.L. Felix, J.R. Meyer, H. Lee, R.U. Martinelli, IEE Proc.: Optoelectron. **150**(4), 351 (2003)
18. M. Brendel, a. Kruse, H. Jönen, L. Hoffmann, H. Bremers, U. Rossow, a. Hangleiter, Appl. Phys. Lett. 99/3 (2011) 031106
19. P.J. Anthony, N.E. Schumaker, J. Appl. Phys. **51**(9), 5038 (1980)
20. M. Yano, J. Appl. Phys. **52**(5), 3172 (1981)
21. R. Olshansky, C. Su, J. Manning, W. Powazinik, IEEE J. Quantum Electron. **20**(8), 838 (1984)
22. J.S. Jang, T.Y. Seong, J. Appl. Phys. 101/1 (2007)
23. D. Mistele, F. Fedler, H. Klausing, T. Rotter, J. Stemmer, O.K. Semchinova, J. Aderhold, J. Cryst. Growth **230**(3), 564 (2001)
24. W. Kim, A. Salvador, A.E. Botchkarev, O. Aktas, S.N. Mohammad, H. Morcoç¸, Appl. Phys. Lett. 69/4 (1996) 559
25. A.R. Goodwin, J.R. Peters, M. Pion, G.H.B. Thompson, J.E.A. Whiteaway, J. Appl. Phys. 46/7 (1975) 3126
26. C.B. Su, J. Schlafer, J. Manning, R. Olshansky, Electron. Lett. **18**(25), 1108 (1982)
27. J. Piprek, Physica Status Solidi (a) **207**(10), 2217 (2010)
28. G.H.B. Thompson, G.D. Henshall, Electron. Lett. **16**(1), 42 (1980)